

Corrosion evaluation and prevention of reactor materials to contain thermochemical material for thermal energy storage

Aran Solé¹, Camila Barreneche^{1,2}, Ingrid Martorell^{1,3}, Luisa F. Cabeza^{1,*}

¹GREA Innovació Concurrent, Universitat de Lleida, Lleida, Spain. Edifici CREA, Pere de Cabrera s/n, 25001, Lleida, Spain. Tel.: +34-973 003576; Fax: +34-973 003575. *lcabeza@diei.udl.cat

²Department of Materials Science & Metallurgical Engineering, Universitat de Barcelona, Martí i Franqués 1-11, 08028 Barcelona, Spain

³Serra Hünter Fellow

*Corresponding author: lcabeza@diei.udl.cat

Abstract

Thermochemical materials (TCM) can be used for seasonal heat storage, storing high amounts of thermal energy coming from the sun in summer and releasing it in winter, when heating for houses is needed. One promising TCM for building comfort applications is the Na₂S/water pair due to its high energy density and appropriate reaction temperature that can be achieved by a solar collector. Nonetheless, Na₂S reacts with oxygen and is corrosive to metals, especially with those used to build up heat exchangers or reactors that contain the TCM. Therefore, corrosion tests in a self-developed experimental setup under vacuum conditions, 13 mbar, between Na₂S·9H₂O/5H₂O and two reactor metals: copper and stainless steel 316 have been performed. Since copper is corroded and is highly used for thermochemical reactors, two promising coatings, Halar and electroless nickel, have been applied. Furthermore, aluminium has also been tested coated with these coatings. Halar is a potential candidate to protect both copper and aluminium heat exchangers/reactor that may contain Na₂S/H₂O pair for thermochemical energy storage. Stainless steel 316 is also corrosion resistant to the selected TCM.

Keywords: Corrosion; Thermal energy storage (TES); Thermochemical material (TCM); Sodium sulphide; Vacuum reactor; Coatings.

32 **1. Introduction**

33 Thermal energy storage (TES) is extremely necessary to match the energy available
34 and the demand. This could lead to thermally independent houses, which would have a
35 positive effect in reducing the global CO₂ emissions. The research in this field is mainly
36 focused on the storage medium and how to implement it in the most efficient way.
37 Several storage materials have been studied, based on different concepts. Sensible,
38 phase change and thermochemical materials are being used to fulfil energy storage
39 requirements depending on the application [1, 2].

40 In this paper the focus is on thermochemical materials (TCM) which undergo a
41 chemical reversible reaction to store and release energy. TCM is an emerging energy
42 storage media with the potential for high-density leading to compact thermal energy
43 storage systems [3] and for high energy efficient systems for energy conversion [4].
44 Moreover, those materials present a huge advantage which remains in almost zero
45 thermal losses to the ambient, since the energy is stored in the form of chemical bonds.
46 Therefore, TCM are suitable for seasonal storage, meaning to provide heat in winter
47 that has been charged in summer. On the other hand, one of the major drawbacks of
48 TCM is that they are corrosive to the reactor/heat exchanger material, usually metal
49 based.

50 Corrosion causes big investment costs, results of one study show that the total annual
51 estimated direct cost of corrosion in the U.S. is a staggering \$276 billion, approximately
52 3.1% of the nation's Gross Domestic Product (GDP) [5]. Hence, corrosion tests should
53 be performed before to ensure long term performance of the equipment containing
54 TCM [6, 7].

55 In a previous study [7] results coming from an experimental corrosion test simulating an
56 open TCM reactor between several TCM and common vessel metals were published.
57 TCM reactors can be open or closed, integrated or non-integrated [8]. Open reactors
58 take the water vapour from the atmospheric air while closed reactors imply that water
59 circulates in a closed loop and is taken from an evaporator and released to a
60 condenser. The later ones can operate under lower or vacuum pressures or inert
61 atmospheres.

62 Some of the most studied TCM work better under low pressures [9] or in an inert or
63 vacuum atmosphere when side reactions have to be controlled [10]. No literature has
64 been found concerning corrosion vacuum tests with TCM. One of the moving forward-
65 preventive strategies for corrosion costs savings is to promote research [5] and thus

66 perform tests seeking for compatible materials and/or preventive solutions like applying
67 coatings [11, 12].

68 There are several types of coating that can protect almost all metals available for
69 engineering use from air, water, acid corrosion, saline ambient, etc. [13]. Those coating
70 are mainly classified as organic [14] and inorganic coatings [15] and the method used
71 to coat the substrates is the main issue under study at this moment.

72 The aim of this study is to develop a device to test corrosion between TCM and metals,
73 under vacuum and controlled temperature. Moreover, experimental corrosion tests
74 have been performed in this setup looking for the suitable material to build up vessels
75 or reactors which contain $\text{Na}_2\text{S}/\text{H}_2\text{O}$ pair as a thermochemical energy storage material.

76 From the recent literature published in this field [1,3,7,8,12] it can be withdrawn the
77 need of more research in order to overcome TCM issues like corrosion, compaction,
78 stability, etc. to promote this technology towards market availability. The contribution of
79 the present study is essential for the design of a reactor/heat exchanger where a TCM
80 reaction for building applications takes place. Although it has been focused on a
81 specific working pair, the designed methodology and setup address a specific step in
82 the reactor design procedure when selecting metals to work in contact with TCM.

83

84 **2. Setup and methodology**

85 **2.1 Setup**

86 The present setup is designed and built to perform corrosion tests simulating closed
87 and integrated TCM reactors. Glass has been selected for being an inert material able
88 to stand high temperatures, low pressures, and allowing direct visual inspection. The
89 design was thought to obtain a versatile, multifunctional device which can operate
90 under a wide range of pressures, temperatures, and different atmospheres, therefore
91 several TCM.

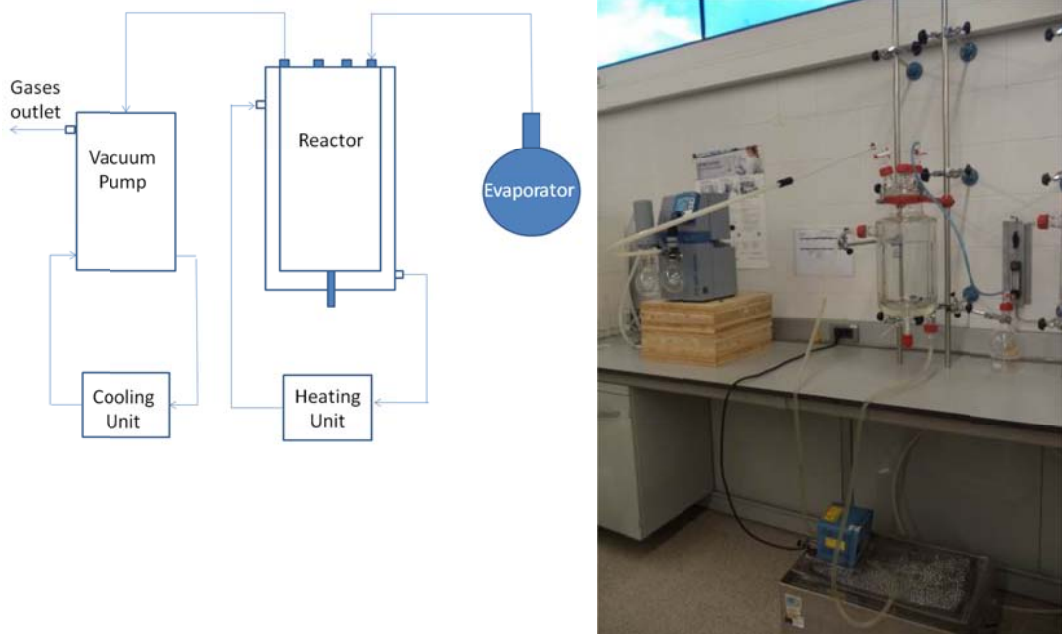
92 A general view of the setup is shown in Figure 1. It consists of a 5 L glass jacketed
93 reactor, connected to a heating unit (thermostatic water bath), an evaporator (round-
94 bottom flask), and a vacuum pump from Vacuubrand PC 600 series. Tubing from the
95 reactor to the vacuum pump is polyamide based connected with common clamps. The
96 reactor contains one open 300 ml vessel to place the TCM and the specimens to be
97 tested (see Figure 2). One temperature sensor is giving the TCM temperature, and
98 another is placed in the atmosphere. Relative humidity (RH) is also measured on-line

101 with a HygroPalm HP22-A. Furthermore, total pressure is measured and controlled by
102 the vacuum pump.

105 The vacuum pump runs in continuous mode, to assure vacuum inside the reactor. The
106 vacuum pump presents an outlet for venting gases, which is directed to the fume hood,
107 being cooled previously (cooling unit) to collect condensed outlet water vapour and
108 other condensable gases.

106

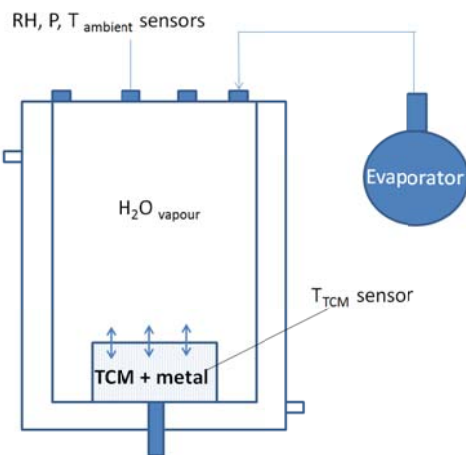
107



108

Figure 1. General view of the setup. Left: scheme, right: picture.

109



110

111

Figure 2. Reactor and evaporator setup sketch.

112

2.2 Methodology

112
113
114
115
116
117
118
119
120
121
122
123
124
125
126
127
128
129
130
131
132
133
134
135
136
137
138
139
140
141
142
143
144
145

For each metal sample, four specimens are needed. One is the reference and the other three are tested for a week in contact with the TCM. The three specimens are replicates in order to ensure the repeatability of the experiments.

To evaluate the results, a methodology accordingly to the setup has been designed. Two different methodologies, one for the single metal specimen and one for the coated metals, are detailed here. First, the metal specimen are cleaned (no polished, no brushed, only acetone). Then, they are weighted in a precision balance (± 0.01 mg) AG135 from Mettler-Toledo and are visually observed by a Zweek optical microscope. The coated specimen are weighted in the same precision balance, but observed in an ESEM Quanta 200 FEI, XTE 325/D8395 scanning electronic microscope (SEM). An SEM is needed for the coated samples since more precision and resolution is required to measure the coating thickness. At this point the methodology merges and three specimens of each sample are placed inside the reactor in a 300 ml vessel fully in contact with the solid $\text{Na}_2\text{S}\cdot 9\text{H}_2\text{O}$. An immersion corrosion test following ASTM G1 [16], under the specified operating conditions determined by the TCM selected, is performed for a week. Before vacuum the reactor, nitrogen gas flows through it to make sure there is no oxygen inside. Finally, the heating unit is connected and set to the established set point.

After the corrosion test, the three specimens are visually inspected, weighted in the same balance and observed in the appropriate microscope. Corrosion processes that go further than the surface level can be identified by both microscopes. Therefore, vessel materials that are not appropriate can be identified. Also, TCM characterization after corrosion tests should be performed (i.e. XRD) to identify the reaction process of the TCM and other possible chemicals.

On the other hand, previous tests were performed to ensure vacuum tightness in the reactor and to check the start-up of the reactor as well as to conduct it to established steady state conditions. Then, tests with only TCM have to be conducted to see the behaviour of the TCM without possible products from corrosion reaction.

The methodology to evaluate corrosion is based on ASTM G1. Corrosion rates are obtained using equation 1 for single metals since ASTM G1 is not adapted to coated metals. Mass loss corresponds to the decrease in mass between before and after (after chemical cleaning, see ASTM G1) the corrosion test.

146

$$CR = \frac{\Delta m}{A \cdot (t_o - t_f)} \quad \text{Eq. 1}$$

147 Corrosion rate CR (mg/cm²·yr) takes into account the mass loss (Δm), the contact area
148 of the metal specimen (A), and the time of exposure ($t_o - t_f$).

149

150 3. Materials

151 3.1 TCM

152

153 A promising TCM, mainly seeking high energy density, has been selected to test and
154 validate the new experimental setup. Sodium sulphide and water pair (Na₂S/H₂O) as a
155 TCM presents a net energy storage value (see Table 1) which is within the best salt
156 hydrates for building applications [17, 18]. Its main drawbacks according to the hazard
157 statements of the Regulation (Ec) 1272/2008 are: toxic if swallowed, it may be
158 corrosive to metals, and in contact with acids liberates toxic gas (H₂S) [19]. Swallowing
159 it can be avoided if the material is kept in a closed vessel as the one designed here.
160 Corrosion can be prevented by coating the metal in contact as it is done in this work.
161 Furthermore, an inert atmosphere or vacuum is needed to prevent sulphites formation
162 and this is why the experimental setup is designed to work under vacuum conditions.

163 The purchased sodium sulphide nonahydrate (Na₂S·9H₂O) is manufactured by Alfa
164 Aesar with 98.0 % purity. Properties associated to the chosen TCM reaction are shown
165 in Table 1.

166 The reaction from nonahydrate to pentahydrate accomplishes the requirement for
167 building applications, a reaction temperature below 100-150 °C achievable by solar
168 collectors and promising net enthalpy values, as shown in Table 1.

169

170 **Table 1. TCM reaction properties for the corrosion vacuum tests.**

$\text{Na}_2\text{S} \cdot 9\text{H}_2\text{O}(\text{s}) \rightarrow \text{Na}_2\text{S} \cdot 5\text{H}_2\text{O}(\text{s}) + 4\text{H}_2\text{O}(\text{v})$	nonahydrate	pentahydrate	Ref
CAS number	1313-84-4	1313-83-3	[19]
Density (g/cm ³)	1.43	1.58	[17]
Melting temperature (°C)	49	83	[17, 20]
Molecular weight (g/mol)	240.184	168.122	[21]

Extrapolated onset temperature (°C)	32.5	[20]
ΔH_r (KJmol ⁻¹)	215±20	[20]
$\Delta H_{net,V^*}$ (KWhm ⁻³)	133	[17]

171 *Includes the volume of the water in the water storage tank

172

173 The reactor operating conditions, which are given by the TCM reaction itself [20], are
 174 shown in Table 2. Everything runs in continuous mode. Water vapour pressure is
 175 always as expected since it is taken from the external evaporator, which is also under
 176 vacuum. Water vapour pressure is also checked by measuring RH and calculating
 177 saturated pressure by Clausius-Clapeyron equation.

178

179

Table 2. Reactor test operating conditions.

Water vapour pressure (mbar)	13
Reactor temperature (°C)	32.5 (dehydration)
Evaporator temperature (°C)	10

180

181 3.2 Metals and coated metals

182

183 The absorption and release of energy coming from the TCM reaction takes place in
 184 reactors. Therefore, heat transfer is needed to be promoted from the TCM to the heat
 185 transfer fluid, usually water for building applications. In that sense prototypes are being
 186 made of high conductivity metals, such as: copper, aluminium, or even stainless steel
 187 316.

188 It is known that there are several materials to be avoided in contact with Na₂S: acids,
 189 oxidizing agents, water/moisture, aluminium/aluminium alloys, copper and air [22].

190

191 In this paper single metals under study are stainless steel 316 and copper. Moreover,
 192 coatings are considered to protect copper and aluminium from Na₂S corrosion. Two
 193 different coatings were chosen, halar (organic coating) and electroless nickel (inorganic
 194 coating). All the pieces dimensions are 6 x 6 x 0.2 cm.

195 Halar® is an organic coating which is mainly composed by Ethylene Chloro
 196 Trifluoroethylene (ECTFE). At temperatures up to 120 °C the polymer is

197 neither affected by stress cracking nor attacked by the majority of chemical reagents.
198 ECTFE is resistant to most chemicals except chlorinated solvents and has better
199 barrier properties to SO₂, Cl₂, HCl, and water than fluorinated ethylene propylene (FEP)
200 and polyvinylidene fluoride (PVDF) [23]. These coatings can be applied with
201 electrostatic powder coating or with spray coating in the slurry formulation which have
202 been described by Choy [24].

203

204 Electroless autocatalytic Nickel-Phosphorus Coatings, from now on electroless nickel,
205 are alloys of nickel and phosphorus produced by autocatalytic chemical reduction with
206 hypophosphite and generally deposited from acid solutions operating at high
207 temperatures. These coatings have multifunctional properties, such as hardness, heat
208 hardenability, abrasion, wear and corrosion resistance, magnetics, electrical
209 conductivity provides diffusion barrier, and solderability [25]. A finishing based on an
210 anticorrosive spray has also been applied onto one copper sample to see if it acts as a
211 protective film against Na₂S.

212

213 **4. Results and discussion**

214 Obtained results from the corrosion test performed to the abovementioned specimen
215 are gathered and shown by, first, single metal specimen which are copper and
216 stainless steel 316, and secondly, by the coated specimen.

217

218 **4.1 Metal specimen**

219 **A) Copper**

220 Corrosion signs were clearly observed in copper specimens, as it can be seen in
221 Figure 3. Black spots (i.e. CuS or/and Cu₂S) on the surface which are products from a
222 side reaction can be clearly observed. The three last pictures (Figure 3, bottom) are
223 from the same specimens after chemical cleaning (following ASTM G1). They present
224 no solid products from corrosion process, but still some surface damage is seen since
225 the surface colour is deteriorated when compared to the initial copper specimen.

226

227

228

229

230

231



Specimen before chemical cleaning process (after corrosion test)



Specimen after chemical cleaning process

234

235

Figure 1. Copper specimen after one week corrosion test with Na₂S. Top: before and bottom: after cleaning.

236

239

240

241

The microscopic section images of the specimen (Figure 4) denote there is no corrosion further than the surface. The lines are due to the cutting process of the specimen.

240



241

Figure 2. Copper section microscopic images before (left) and after (right) corrosion test.

242

246

247

248

249

Corrosion rates (CR) are listed in Table 3. These values of CR belong to the not recommended range ($50\text{-}99\text{ mg cm}^{-2}\text{ yr}^{-1}$) for service greater than a year (see Table 4). When comparing these values with the previously obtained [7] in atmospheric pressure and humidity conditions, it can be concluded that in vacuum, CR value is reduced

246 around 30 times. Nonetheless, for this application copper is not recommended to
 247 contain Na₂S/H₂O, neither in open nor in close configurations. For that reason, it is
 248 remarkable that a coating is needed to protect it before its implementation as part of a
 249 system containing this TCM.

250
 251

Table 3. Initial and final weight of the Cu specimen under study and calculated CR.

	Initial weight (g)	Final weight (g)	CR (mg cm ⁻² yr ⁻¹)
Specimen 1	63.694	63.609	85.54
Specimen 2	63.681	63.601	80.14
Specimen 3	63.727	63.646	81.11

252
 253

Table 2. Guide for corrosion weight loss used in the industry [26].

mg/cm ² yr	Recommendation
>1000	Completely destroyed within days
100–999	Not recommended for service greater than a month
50–99	Not recommended for service greater than 1 yr
10–49	Caution recommended, based on the specific application
0.3–9.9	Recommended for long term service
<0.2	Recommended for long term service; no corrosion, other than as a result of surface cleaning, was evidenced

254
 255

256 **B) Stainless steel 316**

257 Stainless steel 316 did not show corrosion signs after the test. Specimens have the
 258 same appearance as before testing. There are not corrosion effects on the surface.
 259 Moreover, microscopic images (see Figure 5) show that there are not corrosion points
 260 on the surface of the specimens under study. There is no difference at microscope
 261 scale regarding the section surface of the stainless steel specimens under study,
 262 either.

263



Specimens before corrosion test



Specimens after corrosion test

266 **Figure 5. Stainless steel 316 specimens after one week corrosion test with Na₂S. Microscopic images before**
 267 **(top) and after (bottom) corrosion test.**

267

272 Corrosion rate values are shown in Table 5, which are inside recommended range for
 273 long term service (see Table 4). CR values in this case are in the same range as the
 274 obtained under atmospheric pressure and humidity conditions [7]. Therefore, stainless
 275 steel 316 corrosion compatibility with Na₂S/H₂O is not influenced by the working
 276 atmosphere (e.g. air and vacuum).

273

274 **Table 3. Initial and final weight of the stainless steel 316 specimens under study and calculated CR.**

	Initial weight (g)	Final weight (g)	CR (mg cm ⁻² yr ⁻¹)
Specimen 1	80.804	80.800	4.34
Specimen 2	81.046	81.041	5.05
Specimen 3	80.883	80.878	4.44

275

282 Stainless steel 316 is a potential candidate as it has been experimentally tested under
 283 the real operating conditions and the results recommend it for long term service;
 284 nevertheless there are also other aspects to take into account when selecting a
 285 material vessel to build up a heat exchanger or a reactor. Heat transfer should not be
 286 limiting in a TCM reactor since then thermal power output of the reactor/heat
 287 exchanger would be lower than expected. Since a coating layer represents an
 288 additional thermal resistance in the heat transfer during reaction, experiments are

282 suggested to be carried out to reveal to which extent the thermal performance of the
283 heat exchanger is decreased by the coating.

284

285 **4.2 Coated specimens: halar® and electroless nickel**

286 **A) Copper coated with halar®**

287

288 Figure 6 shows the SEM images captured for each Cu-specimen tested under vacuum
289 corrosion test and one reference. The images correspond to the cross section of the
290 specimens under study where the halar® coating can be seen in the upper side.

291 SEM images revealed that the coating thickness remains constant and is exactly the
292 same (around 190-200 μm) as it is observed in Figure 6. The coating thickness
293 remains almost constant regardless of the specimen. Therefore, copper coated with
294 halar® is corrosion resistant to $\text{Na}_2\text{S}/\text{H}_2\text{O}$ pair and can be used when copper is needed
295 as a base metal.

296

297

298

299

300

301

302

303

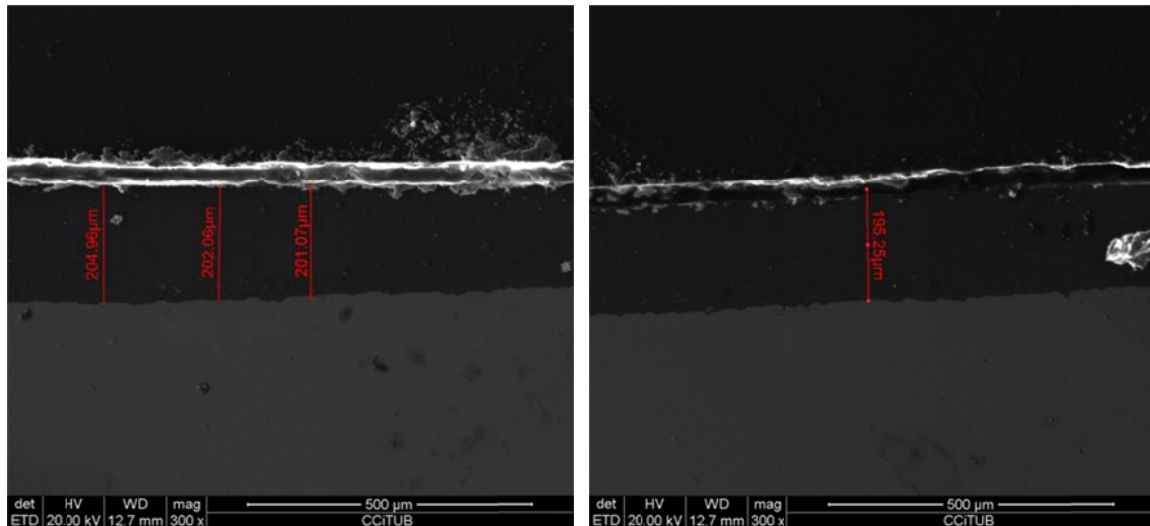
304

305

306

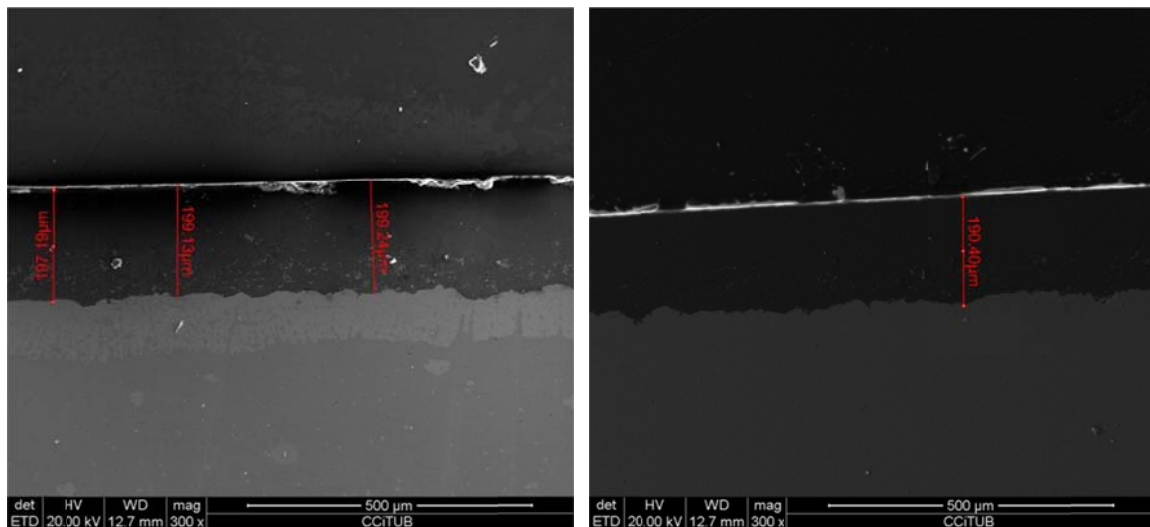
307

308



Reference

Specimen 1



Specimen 2

Specimen 3

310 Figure 6. Copper specimens coated with halar®.

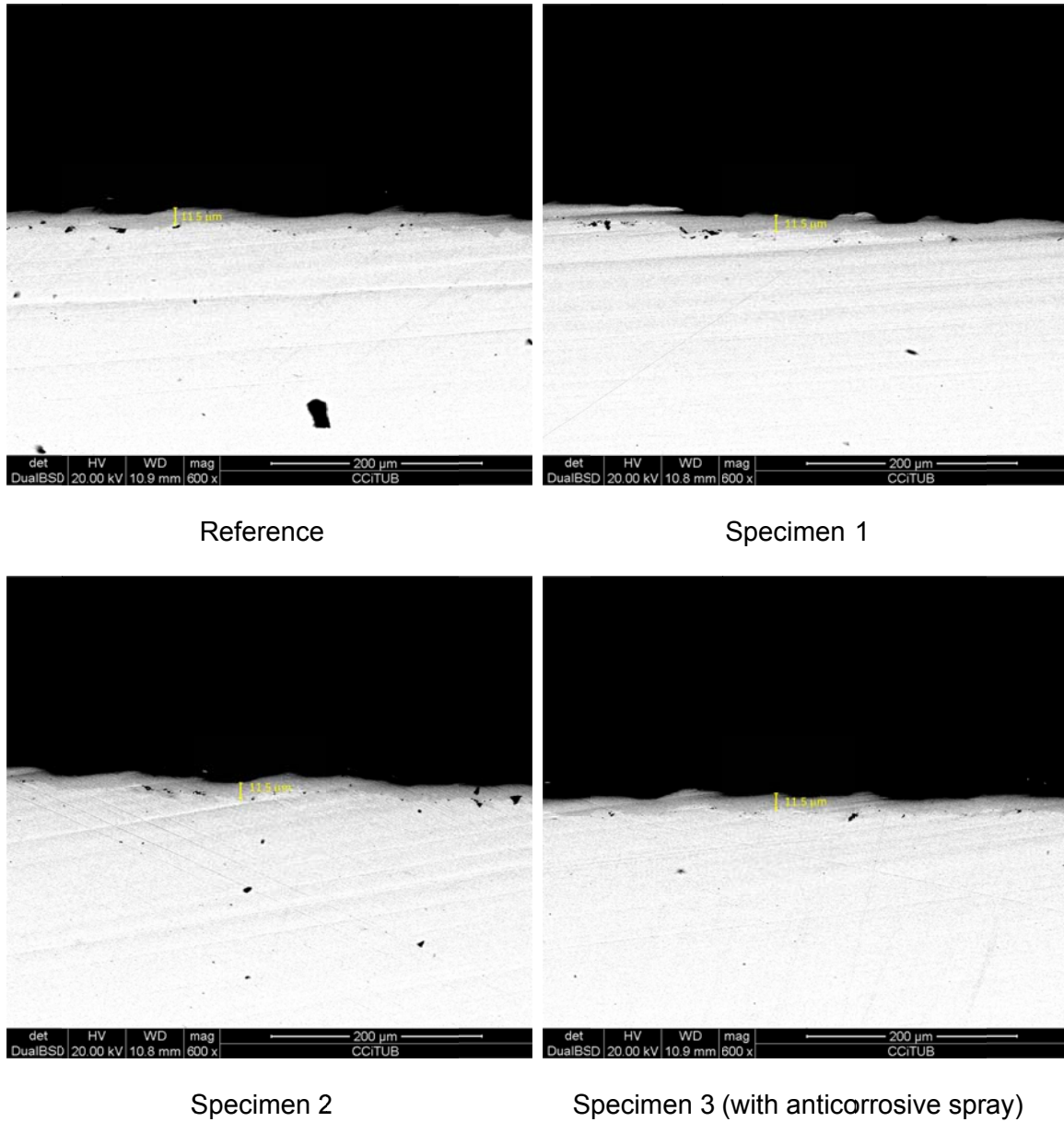
311

312 **B) Copper coated with electroless nickel**

324 Figure 7 shows the coating of the specimens coated with Ni-electroless technique.
 325 There is one specimen without being tested (the reference), there are two specimens
 326 coated with Ni-electroless coating and there is one specimen that has the same coating
 327 and also a finish anticorrosive and non-sticked spray (M3). The samples morphology is
 328 shown in the SEM using secondary electrons. However, the backscattered electrons
 329 are able to provide composition information of the displayed sample: the darker the
 330 sample the lighter the atoms are. Thus, the morphology of the Aluminium + electroless
 331 Ni samples is very similar and secondary electrons are unable to differentiate the
 332 sample and the coating. In addition, backscattered electrons not clarify much the
 333 difference between sample and coating because Ni and Al have very similar atomic
 334 weight. Thereby, SEM images are not very enlightening, although the thickness of the
 335 coating layer is distinguished. Figure 7 shows that there is no corrosion and the

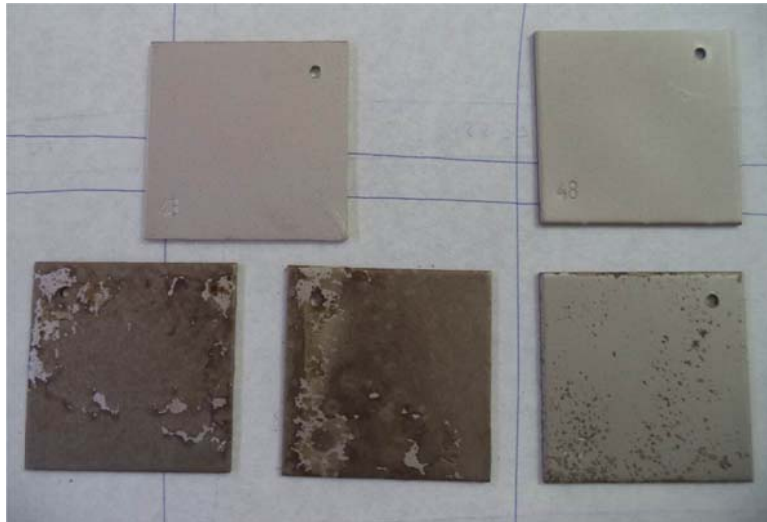
329 thickness of the coating is the same for all the specimens under study after one week
330 of vacuum corrosion testing. Nonetheless, pictures taken at surface level, after the test,
331 show clear damage (Figure 8), even more when this anticorrosive spray is not applied
332 on the specimen. The spray applied is useful to avoid the oxide formation on the
333 surface of the sample under study.

330



331

Figure 7. Copper specimens coated with Ni electroless coating



332

335
336
337
336

Figure 8. Copper specimens coated with Ni electroless coating. First two top are reference without spray and reference with anticorrosive spray. Bottom, three tested specimens, first two without spray, and the third with spray.

337

C) Aluminium coated with halar®

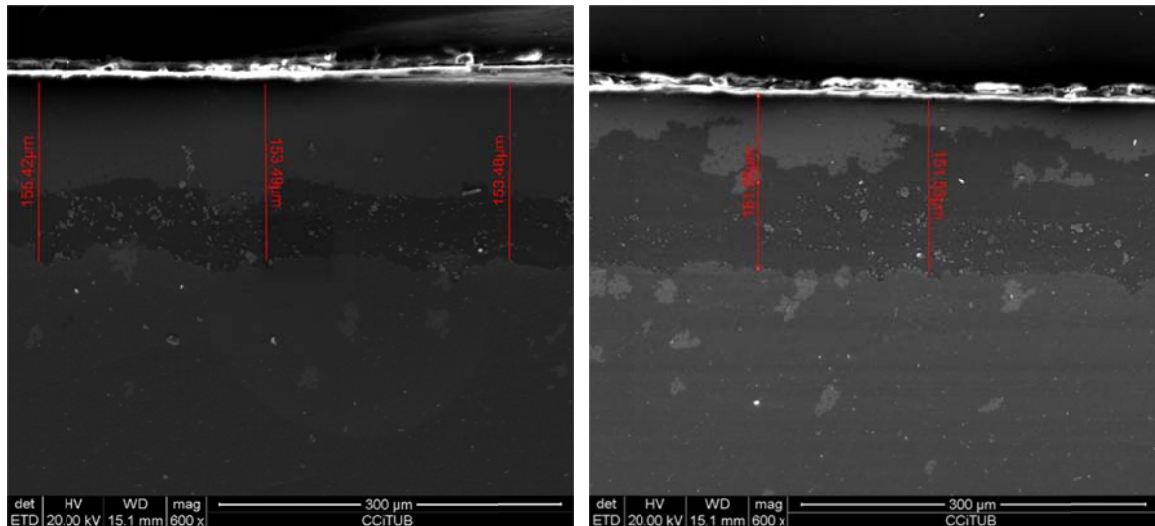
340
341
342

Figure 9 shows the SEM images captured for each specimen tested under vacuum corrosion test and one reference. The images show the cross section of the specimens under study where halar® coating is shown in the upper side.

344
345
346
347

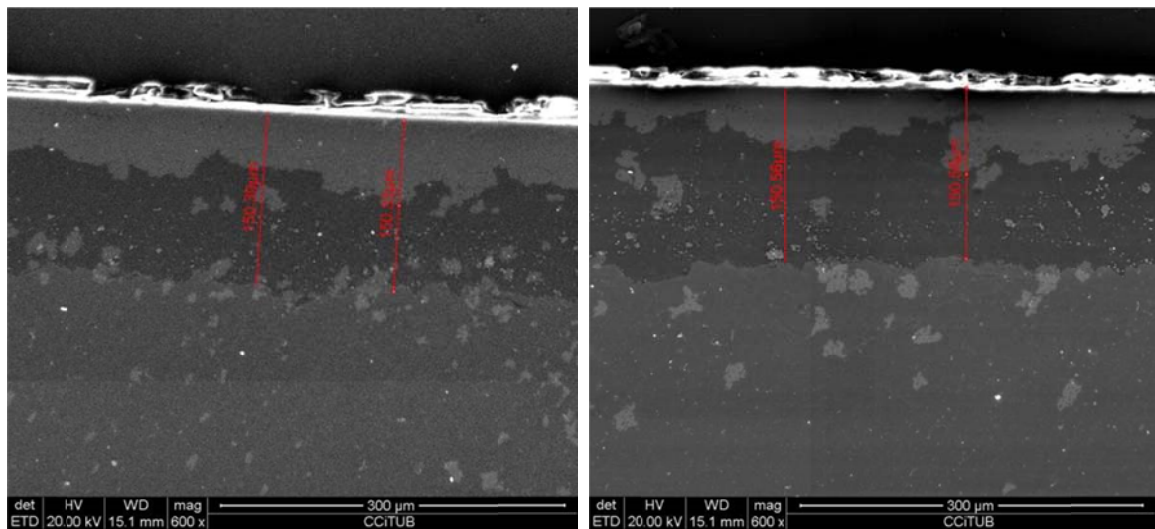
SEM images revealed that the coating size is exactly the same (around 150 μm) as it is observed in Figure 9. Since neither paths nor holes produced from corrosive products from the TCM are observed, this coating is recommended to be used when in contact with $\text{Na}_2\text{S}/\text{H}_2\text{O}$ pair.

345



Reference

Specimen 1



Specimen 2

Specimen 3

Figure 9. Aluminum specimens coated with halar.

346

347

348

349

D) Aluminium coated with electroless nickel

356

Results of SEM images of aluminium specimens coated with nickel can be seen in

357

Figure 10. Nickel coating shows a non-flat surface which is in contact with the metal.

358

This fact makes difficult the comparison of the coating thickness. Nevertheless, it can

359

be observed that no corrosion sign is seen since any degradation of the coating,

360

neither inner paths are formed. When specimens are observed visually, as Figure 11, it

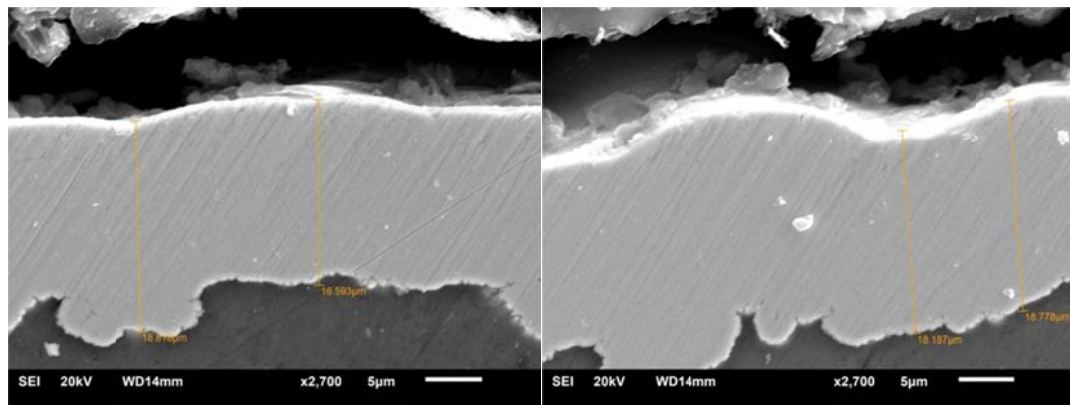
361

can be seen that surface is damaged. Therefore, this coating is damaged by Na_2S

362

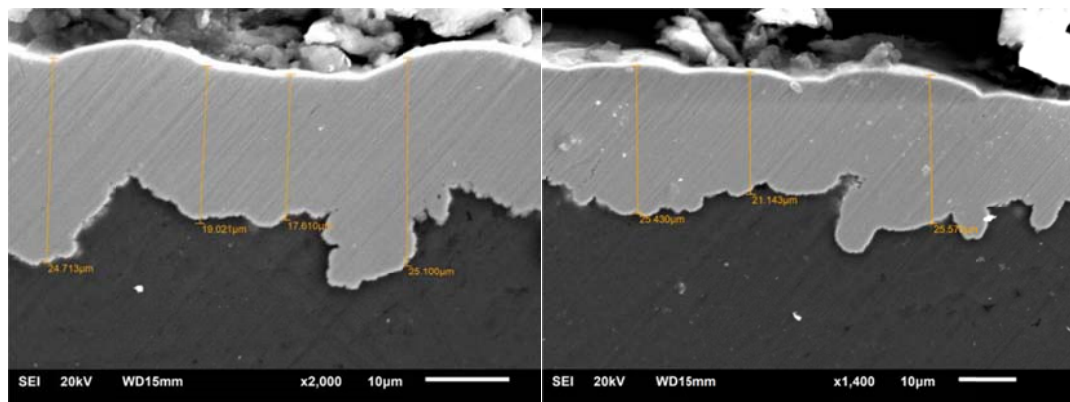
reaction only at surface level.

357



Reference

Specimen 1



Specimen 2

Specimen 3

Figure 10. Aluminium specimens coated with Ni electroless coating, SEM.

358
359



Figure 11. Aluminium specimens coated with Ni electroless coating. On the top, the reference, on the bottom, the three tested specimens.

360
362
363
363

4.3 Na₂S XRD after corrosion vacuum test

368 X-ray diffraction (XRD) analysis was performed to the TCM after the corrosion vacuum
369 test. This technique shows the crystalline phases that composed the samples.
370 Therefore, the XRD spectrum identifies the crystalline sample components. However, it
371 does not discern the main component, neither quantifies each detected substance.

368 Here, the aim is to corroborate that the reaction from the nonahydrate to the
369 penthydrate has taken place when performing the vacuum tests. This would imply the
370 appearance of the pentahydrate characteristic peaks in the XRD results.

371 The XRD spectrum shows that there are three main crystalline substances in this
372 sample: $\text{Na}_2\text{S}\cdot 5\text{H}_2\text{O}$, $\text{Na}_2\text{S}\cdot 9\text{H}_2\text{O}$ and Na_2SO_3 . Na_2SO_3 appears in the composition due
373 to the atmosphere contact during the sample preparation and extraction in the
374 corrosion reactors.

375

376 **4 Conclusions**

377 A setup composed by a 5 L glass jacketed reactor, evaporator, and a vacuum pump
378 has been developed at lab scale to test corrosion of thermochemical materials under
379 different atmospheres and a wide range of pressure and temperature. A new
380 methodology to perform these tests has been designed, explained in detailed, tested
381 and validated.

382 One TCM pair, $\text{Na}_2\text{S}/\text{H}_2\text{O}$, has been selected to perform vacuum corrosion tests at 13
383 mbar and 32.5 °C when in contact with commonly used metals and coated metals used
384 to build up thermochemical reactors.

385 From the screening corrosion vacuum tests performed with the TCM reaction from the
386 nonahydrate to the pentahydrate sodium sulphide it can be concluded that copper is
387 not recommended to contain $\text{Na}_2\text{S}/\text{H}_2\text{O}$, neither in open nor in close configurations,
388 besides that in closed and vacuum corrosion rate value is reduced by 30 times. In the
389 case of stainless steel 316 results show that is recommended for long term service.

390 Two coatings have been tested when applied onto copper and aluminium, two metals
391 highly used for the manufacturing of TCM heat exchangers. Halar coating results make
392 it a potential candidate to be selected to protect heat exchangers/reactor that may
393 contain $\text{Na}_2\text{S}/\text{H}_2\text{O}$ pair for thermochemical energy storage. Electroless nickel shows no
394 corrosion when observing SEM images, but it is visually damaged at surface level after
395 the corrosion test. When a finishing spray is applied it improves the material resistance
396 against corrosion.

397 Moreover, further tests are suggested to carry out to ensure that the materials which do
398 not present corrosion can resist for longer periods. Also, heat transfer coefficient
399 should be measured with the selected metal or coated metal to ensure that heat
400 transfer is not the limiting step in the reactor.

401 **Acknowledgements**

402 The research leading to these results has received funding from the European
403 Commission Seventh Framework Programme (FP/2007-2013) under grant agreement
404 No ENER/FP7/295983 (MERITS). Aran Solé would like to thank the Departament
405 d'Universitats, Recerca i Societat de la Informació de la Generalitat de Catalunya for
406 her research fellowship. The work is partially funded by the Spanish government
407 (ENE2011-22722). The authors would like to thank the Catalan Government for the
408 quality accreditation given to the research group GREA (2014 SGR 123).

409

410 **References**

- 411 [1] International Energy Agency, Technology Roadmap, Energy Storage, 2014.
- 412 [2] C.W. Chan, J. Ling-Chin, A.P. Roskilly. Reprint of “A review of chemical heat pump,
413 thermodynamic cycles and thermal energy storage technologies of low grade heat
414 utilisation”. Appl. Therm. Eng. 53 (2013) 160-176.
- 415 [3] M.A. Rosen, Energy Storage, Nova Science Publishers, Hauppauge, New York,
416 2012.
- 417 [4] Y. Aristov, D.M. Chalaev, B. Dawoud, L.I. Heifets, O.S. Popel, G. Restuccia,
418 Simulation and design of a solar driven thermochemical refrigerator using new
419 chemisorbents, Chem. Eng. J. 134, 1, (2007) 58-65.
- 420 [5] <https://www.nace.org/Publications/Cost-of-Corrosion-Study/> (last accessed
421 06/06/15)
- 422 [6] E. Opila, High temperature materials corrosion challenges for energy conversion
423 technologies, Electrochemical Society Interface 22 (2013) 69-73.
- 424 [7] A. Solé, L. Miró, C. Barreneche, I. Martorell, L. F. Cabeza, Corrosion of metals and
425 salt hydrates used for thermochemical energy storage, Renew. Energ. 75 (2015) 519-
426 523.
- 427 [8] A. Solé, I. Martorell, L. F. Cabeza, State of the art on gas-solid thermochemical
428 energy storage systems and reactors for building applications, Renew. Sust. Energ.
429 Rev. 47 (2015) 386-398.

- 430 [9] V.M. Van Essen, J. C. Gores, L.P.J. Bleijendaal, H.A. Zondag, R. Schuitema, M.
431 Bakker, W.G.J. van Helden, Characterization of salt hydrates for compact seasonal
432 thermochemical storage, 3rd International Conference of Energy Sustainability 2009,
433 San Francisco, USA, 19-23 July 2009.
- 434 [10] X. Fontanet, Estudio del Na₂S como material de almacenamiento termoquímico.
435 University of Barcelona. Graduate Thesis. 2013.
- 436 [11] A. Frankel, G. Grundmeier, H. McMurray, T. Shinohara, Coatings for corrosion
437 protection, The electrochemical society, New Jersey, US, 2010.
- 438 [12] A-J. de Jong, R. Stevens, C. Rentrop, C. Hoegaerts, Coating development for
439 thermochemical heat storage reactors, International Conference on Solar Heating and
440 Cooling for Buildings and Industry, SHC 2014, Beijing, China, 2014.
- 441 [13] S.L. Shawla, R.K. Gupta, Material selection for corrosion control, ASM
442 International, US, 2010.
- 443 [14] A. Forsgren, Corrosion Control through Organic Coatings, CRC Press, Taylor and
444 Francis Group, US, 2006.
- 445 [15] J. R. Davis, Corrosion: Understanding the Basics, ASM International, US, 2000.
- 446 [16] ASTM G1-03, Standard for Preparing, Cleaning, and Evaluating Corrosion Test
447 Specimens. 2003.
- 448 [17] K. E. N'Tsoukpoe, T. Schmidt, H. U. Rammelberg, B. A. Watts, W.K.L. Ruck, A
449 systematic multi-step screening of numerous salt hydrates for low temperature
450 thermochemical energy storage, Appl. Energ. 124 (2014) 1-16.
- 451 [18] A-J. de Jong, F. Trausel, C. Finck, L. Van Vilet, R. Cuypers, Thermochemical heat
452 storage – system design issues, International Conference on Solar Heating and
453 Cooling for Buildings and Industry, SHC2013, Freiburg (Germany), Energy Procedia 48
454 (2014) 309-319.
- 455 [19] www.solvaychemicals.us (last accessed 06/06/15)
- 456 [20] R. De Boer, W.G. Haije, J.B.J. Veldhuis, Determination of structural,
457 thermodynamic and phase properties in the Na₂S-H₂O system for application in
458 chemical heat pump, Thermochim. Acta 395 (2003) 3-19.
- 459 [21] D. L. Perry, Handbook of inorganic compounds, second ed., CRC Press, 2011.

- 460 [22] www.alfa.com/msds/british/11664.pdf (last accessed 06/06/2015)
- 461 [23] M. Kutz, Applied Plastics Engineering Handbook: Processing and Materials, Hand
462 Book Series, Elsevier, US, 2011.
- 463 [24] K.L. Choy, Chemical vapour deposition of coatings, Prog. Mater. Sci. 48, 2 (2003)
464 57–170.
- 465 [25] ASTM B 733 – 97, Standard Specification for Autocatalytic (Electroless) Nickel-
466 Phosphorus Coatings on Metal, 1997.
- 467 [26] V.S. Sastri, E. Ghal, M. Elboudjaini, Corrosion, prevention and protection. Practical
468 solutions, John Wiley & Sons, Chichester, UK, 2007.